Synthesis and Spectroscopic and Electrochemical Characterisation of a Conducting Polythiophene Bearing a Chiral β-Substituent: Polymerisation of (+)-4,4′-Bis[(*S*)-2-methylbutylsulfanyl]-2,2′-bithiophene

Dario Iarossi,[a] Adele Mucci,*[a] Francesca Parenti,[a] Luisa Schenetti,*[a] Renato Seeber,[a] Chiara Zanardi,[a] Arrigo Forni,[a] and Massimo Tonelli[b]

Abstract: A regioregular *head-to-head/tail-to-tail* poly(β,β′-disubstituted bithiophene) **P1** was synthesised by chemical and electrochemical polymerisation of 2,2′-bithiophene that bears (*S*)-2-methylbutylsulfanyl chains in the β and β′-positions. The polymer was characterised by GPC, NMR and UV/Vis spectroscopy, CD, AFM and by electrochemical and conductivity measurements. The CD spectra of **P1** in solutions in which poor solvents are present show interesting features and allow the presence of different optically active species to be distinguished. Upon varying the casting conditions of **P1**, different relative amounts of grainy and homogeneous aggregated phases were observed in AFM micrographies of films and corresponding negative or positive first Cotton effects were found in the CD spectra. AFM, CD and UV/Vis characterisations were also performed on an electrogenerated optically active polymer **PE1**, in order to make a comparison with the chemically synthesised one. The interesting, small band gap of **P1** allows for easy p- and n-electrochemical doping.

Keywords: aggregation · circular dichroism · electrochemistry · polymers · scanning probe microscopy · thin films

Introduction

Polythiophenes (PTs) that have β-substituents have, for the last few years, constituted one of the most interesting classes of conductive polymers. They have attracted great interest due to their potential application in the field of secondary batteries, electronic and electro-optical devices and electrochemical sensors.[1] Poly(β-substituted thiophene)s can be chemically or electrochemically synthesised from the corresponding β-substituted thiophenes or β,β′-disubstituted bithiophenes.[1] Their physical properties are strongly dependent on the regiochemistry; for example, a greater increase in conductivity upon doping is observed in regioregular *head-to-tail* (HT) PTs compared with regiorandom PTs.[2]

This is one reason why two of the first steps in the characterisation of PTs are usually the correct identification of the regiochemistry of the polymer and evaluation of the molecular-weight distribution. The former goal can be achieved through the judicious use of two-dimensional heterocorrelated NMR experiments in inverse detection,[3] while the latter is usually obtained through Gel Permeation Chromatography (GPC) by using a calibration curve of monodisperse polystyrene standards. Investigation of the electrical, electro-optical and electrochemical properties represents a further step in relation to possible applications of these materials in the field of electro-optical or electronic devices, or electrochemical sensors. An additional target is gaining insight into the correlation between the structure and properties of PTs by studying the intramolecular and supramolecular architecture of this class of materials. A number of recent studies on the aggregation of PTs can be considered in this light.[4–6] Among them, those dealing with the introduction of chiral pendant groups at the β-positions of the thiophene moiety[4, 5] particularly attracted our attention. Enantiomerically pure side chains can, in fact, induce main-chain chirality into the thiophene backbone. This permits the observation of chiro-optical properties,[1a] in addition to solvatochromic and thermochromic properties, that can be utilised to extract information on the organisation of the polymer chains.

In this paper, we report on the synthesis and characterisation of polymers **P1** and **PE1**, obtained by the oxidative ($FeCl_3$) and electrochemical polymerisation of (+)-4,4′-bis[(*S*)-2-methylbutylsulfanyl]-2,2′-bithiophene (**1**). Morpho-

[a] Dr. A. Mucci, Prof. L. Schenetti, Prof. D. Iarossi, Dr. F. Parenti, Prof. R. Seeber, Dr. C. Zanardi, Prof. A. Forni
Dipartimento di Chimica, Università di Modena e Reggio Emilia
Via Campi 183, 41100 Modena (Italy)
Fax: (+39) 59-373543
E-mail: mucci.adele@unimo.it
schene@unimo.it

[b] Dr. M. Tonelli
Centro Interdipartimentale Grandi Strumenti
Università di Modena e Reggio Emilia
Via Campi 213A, 41100 Modena (Italy)

0947-6539/01/0703-0676 $ 17.50+.50/0

logical studies through atomic force microscopy (AFM) of films cast on mica or electrodeposited on Pt electrodes were added to the classical approaches to characterisation (GPC, NMR Spectroscopy, UV/Vis spectroscopy, Circular Dichroism (CD), electrochemical and conductivity measurements) to extract further information on the macromolecule aggregation.

Results

Chemical synthesis: Polymer **P1** was obtained through oxidative polymerisation of dimer **1** with $FeCl_3$ (Scheme 1). The synthesis of **1** (Scheme 2) was carried out from the corresponding dibromo derivative through bromine–lithium exchange with butyl lithium, followed by reaction with (+)-bis[(*S*)-2-methylbutyl]disulfide.[7] Disulfide was obtained from the corresponding thioacetate,[8] derived from (*S*)-(−)-2-methylbutane-1-ol, through a bromination step to (*S*)-(+)-1-bromo-2-methylbutane.

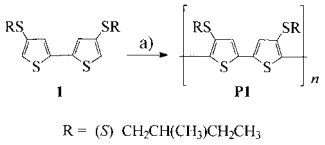

Scheme 1. a) $FeCl_3$, $CHCl_3/CH_3NO_2$ (1:1), 20 h RT (59% **P1**).

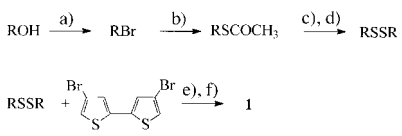

Scheme 2. a) PBr_3, pyridine, 0 °C. b) AcSH, Et_3N, 1,2-dimethoxyethane, 1 h reflux. c) NaOH, $EtOH/H_2O$ (1:1), 1 h reflux. d) Pentane, I_2, RT. e) BuLi, THF/hexane, −60 to −50 °C. f) THF, −5 to 0 °C.

Molecular weight determination: The weight-average molecular weight, M_w, and number-average molecular weight, M_n, of **P1** were 50000 and 17000 ($D = 2.9$), respectively.

NMR characterisation: The ^{1}H NMR spectrum of **P1** (Figure 1a) has a peak at $\delta = 7.19$, in the aromatic region, due to H3 proton of the thiophene ring. The aliphatic region shows seven groups of signals that can be attributed to the protons of the alkylsulfanyl chain. The ^{13}C chemical shifts were detected and assigned through heteronuclear multiple quantum coherence (HMQC) experiments,[9] with an evolution delay of 50 ms (Figure 1b). This evolution delay allows for the detection of all four of the aromatic H,C correlations (both direct and long range). Discrimination among the different carbon signals is based on the coupling constant J(H,C) values and on the long-range correlation detected between SCH_2 protons and the aromatic carbon bearing the alkysulfanyl chain. The ^{1}H and ^{13}C data of **P1** are reported in Table 1. Aromatic proton and carbon chemical shifts are very close to those reported for poly[4,4′-bis(alkylsulfanyl)-2,2′-bithiophene]s,[10] as expected given that they have the same *head-to-head/tail-to-tail* (HH/TT) regiochemistry.

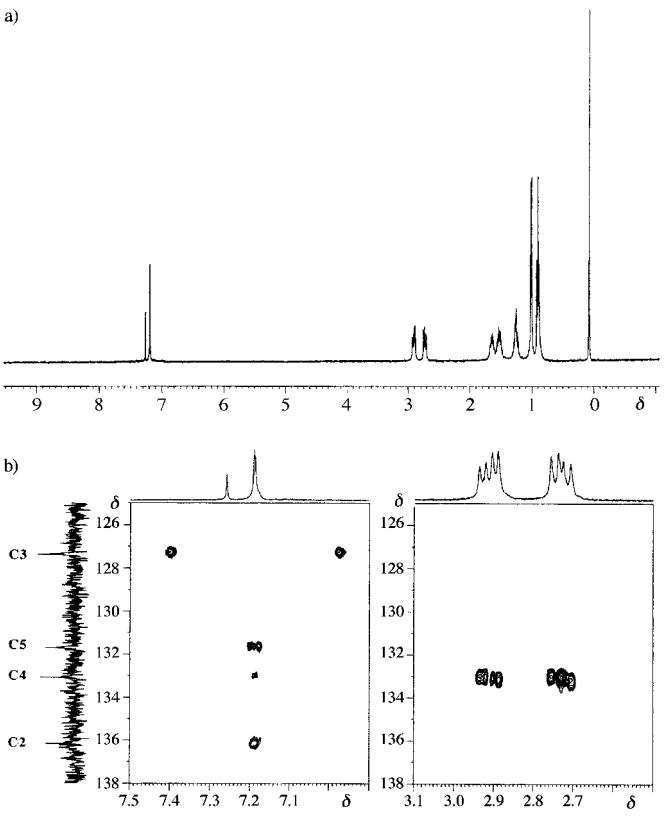

Figure 1. a) ^{1}H NMR spectrum of **P1**. b) HMQC spectrum of the aromatic region of **P1**, 50 ms evolution delay.

Table 1. ^{1}H and ^{13}C Chemical Shifts (in ppm) of **P1**.

	H3			C1′-H_2	C2′-H	C3′-H_2	C4′-H_3	C2′-H_3
	7.19			2.91/2.73	1.64	1.52/1.25	0.89	1.00
C2	C3	C4	C5	C1′	C2′	C3′	C4′	C2′-H_3
136.1	127.4	133.0	131.7	43.5	34.9	28.6	11.3	18.9

Infrared spectroscopy: The native polymer was analysed with an IR microscope. The alkylsulfanyl chain gives rise to stretching vibrations in the region 2960–2850 cm^{-1} and to deformation modes around 1474, 1430 (S−CH_2) and 1377 cm^{-1}. The aromatic (C−H)β stretching and out-of-plane deformation were found at 3074 and 817 cm^{-1}, respectively. The thiophene ring stretching contributes to the band at 1474 cm^{-1}.

UV/Vis and CD spectroscopy: UV/Vis and CD spectra of **P1** in different solvent mixtures are shown in Figures 2 and 3. The solvatochromic behaviour, as shown by the UV/Vis spectra of **P1** (Figure 2b) in chloroform/methanol mixtures, is very similar to that observed for poly[4,4′-bis(alkylsulfanyl)-2,2′-bithiophene]s[10] and for regioregular HT poly(3-alkylthiophene)s.[4a, 4c, 11] An absorption maximum is present in chloroform solution at 469 nm; this is associated with the $\pi-\pi^*$ transition, whereas a red-shifted band, characterised by vibronic structure (with three new maxima at 530, 565, 623 nm), appears when increasing amounts of methanol are added. Correspondingly, a change in colour from orange to violet is observed. The $\pi-\pi^*$ transition at $\lambda_{max} = 469$ nm is

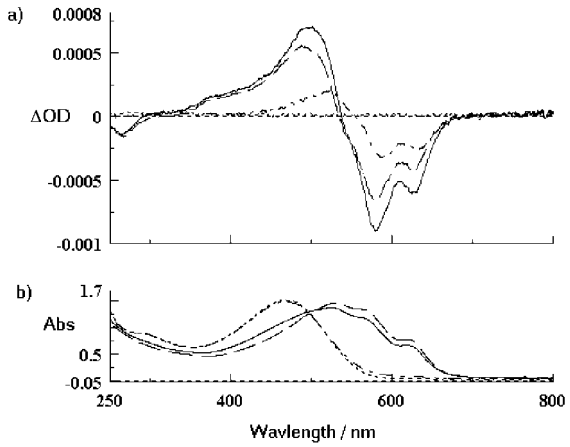

Figure 2. a) CD and b) UV/Vis spectra of **P1** in chloroform/methanol mixtures: 10:1 (••••), 8:2 (•–•–), 7:3 (——), 6:4 (- - - -).

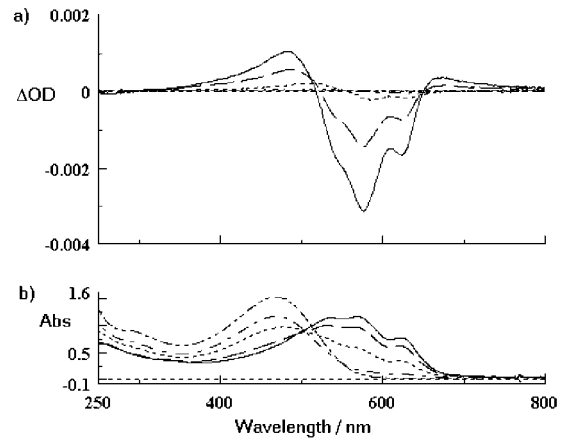

Figure 3. a) CD and b) UV/Vis spectra of **P1** in chloroform/*n*-hexane mixtures: 10:1 (-·····-), 5:5 (•–•–), 4:6 (••••), 3:7 (- - - -), 1:9 (——).

optically inactive in chloroform (Figure 2a). However, upon increasing the amount of methanol, a bisignate Cotton effect (CE) is observed at longer wavelengths. Comparison of the spectra in Figures 2a and 2b shows that the CE does not parallel UV/Vis solvatochromism. The CE shows its maximum negative g ($\Delta A/A$) value (-1×10^{-3} at $\lambda=638$ nm) in chloroform/methanol 7:3, whereas the maximum of the red-shifted vibronic band is further enhanced at a ratio of 6:4. An accurate analysis of the spectra shows that the shape of CE changes when passing from a chloroform/methanol ratio of 8:2 to 7:3, but remains the same from 6:4 onwards.

Interestingly, solvatochromic behaviour is also observed when a poor apolar solvent, such as *n*-hexane, is employed. The UV/Vis spectra of **P1** (Figure 3b) in chloroform/*n*-hexane mixtures are very similar to those in mixed chloroform/methanol solvents. In this case the three maxima of the red-shifted band (that appears when increasing amounts of *n*-hexane are added) are found at 538, 570 and 626 nm. The corresponding CD spectra show a trend similar to that previously found in chloroform/methanol mixtures. Firstly, at a 4:6 chloroform/*n*-hexane ratio, a bisignate CE, very similar to that found at the 8:2 chloroform/methanol ratio, appears but for increasing amounts of *n*-hexane a further positive CE band is observed at 669 nm; this does not correspond to a significant UV/Vis absorption band. Comparison of the spectra in Figures 3a and 3b shows that CE parallels UV/Vis solvatochromism in chloroform/*n*-hexane mixtures with a maximum negative g factor of -3×10^{-3} at $\lambda=578$ nm at 1:9 ratio.

CD and UV/Vis spectra corresponding to minimum and maximum optical activity in both chloroform/methanol and chloroform/*n*-hexane mixtures are compared in Figures 4 and 5. By comparing the spectra, we can infer that at a high chloroform/poor solvent ratio, the same optically active

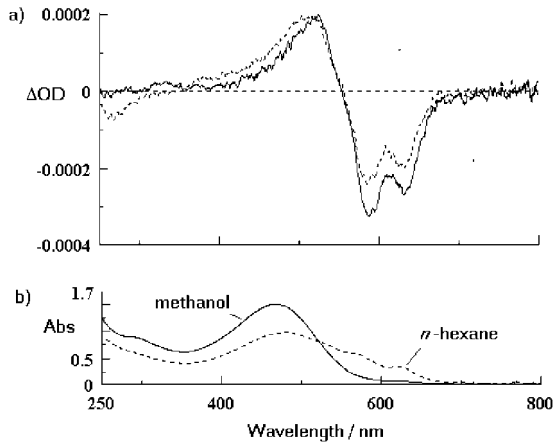

Figure 4. a) CD and b) UV/Vis spectra of **P1** in chloroform/methanol 8:2 and chloroform/*n*-hexane 4:6 mixtures.

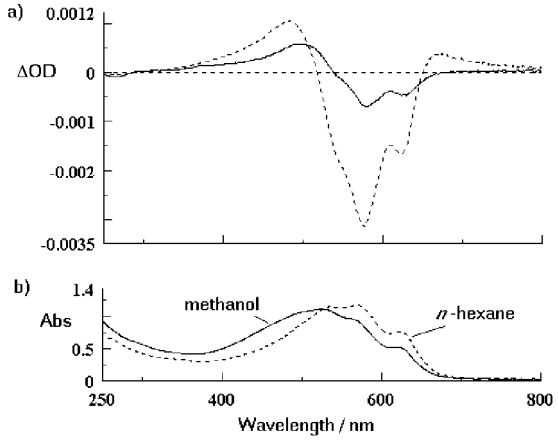

Figure 5. a) CD and b) UV/Vis spectra of **P1** in chloroform/methanol 7:3 and chloroform/*n*-hexane 1:9 mixtures.

species are formed in both mixtures, whereas the markedly different UV/Vis spectra suggest a different degree of order. In both cases, further additions of the poor solvent induce different changes in the two CD spectra and greater similarity between the two UV/Vis spectra (Figure 5). In particular, we observed the presence of a positive CE at 669 nm in chloroform/*n*-hexane, which is undetectable in chloroform/methanol, and a major blue-shift of about 10 nm of the second positive band. In addition, the CE induced by adding *n*-hexane is globally higher than that observed when methanol had been added.

0947-6539/01/0703-0678 $ 17.50+.50/0 *Chem. Eur. J.* **2001**, *7*, No. 3

We have also investigated the CD behaviour of **P1** films cast onto glass from chloroform and THF solutions under different evaporation rate conditions (see Experimental Section). Figure 6 shows two CD and UV/Vis spectra

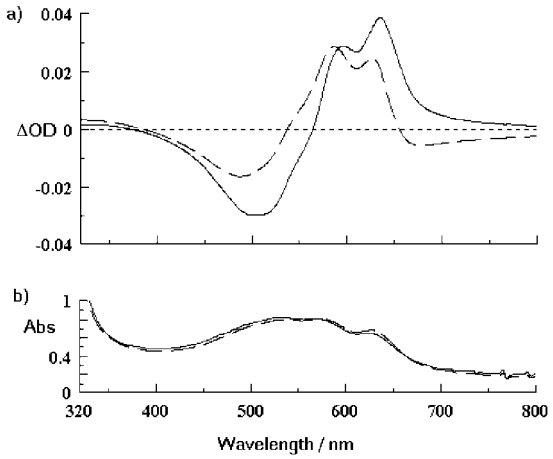

Figure 6. a) CD and b) UV/Vis spectra of **P1** films cast from chloroform under slow evaporation conditions.

obtained by casting from chloroform solution at a slow rate of evaporation (>20 min). To allow for different film thicknesses the spectra are normalised with respect to UV/Vis absorptions. Under these conditions, the maximum *g* factor is around $+6\times10^{-2}$ at $\lambda=639$ nm (solid line), which is among the highest values reported for chiral PTs in the literature.[4a, 4d] It is, however, apparent that, although very similar to each other, the two spectra are not identical in shape, even if the casting conditions were intended to be the same. The CD spectrum of the film cast from chloroform solution under fast evaporation conditions (Figure 7, solid line) is opposite in sign (maximum *g* factor equal to -3×10^{-3} at $\lambda=648$ nm), but not an exact mirror image of the former ones (Figure 6). When

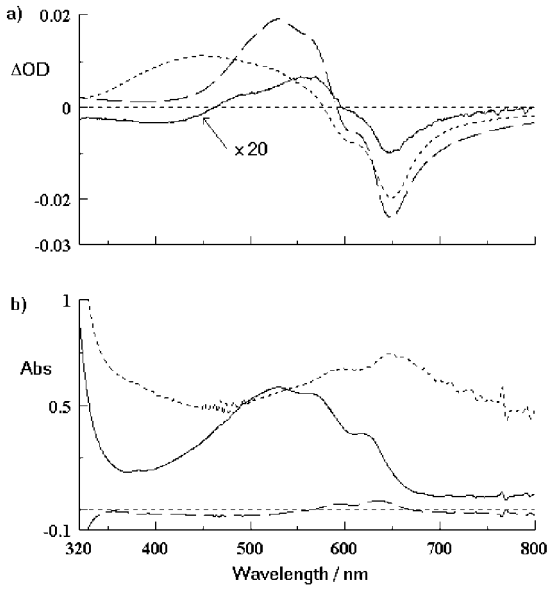

Figure 7. a) CD and b) UV/Vis spectra of film fast cast from chloroform solution (——); film cast slowly from THF solution (••••); difference between the spectra of Figure 6 (- - - -).

casting slowly (>20 min) from THF solution, a very similar CD spectrum (Figure 7, dotted line) to that obtained by fast casting from chloroform (Figure 7, solid line) is obtained, with a *g* factor that reaches the value of -8×10^{-2} at $\lambda=650$ nm. It is worth noting that the corresponding UV/Vis spectra are different. Two well distinguishable maxima, at 590 and 650 nm, are present in the UV/Vis spectrum recorded by casting from THF (affected by light diffusion owing to the presence of an aggregate phase and shown by optical-microscope inspection). Both are red-shifted with respect to the first two vibronic bands, at 565 and 619 nm, of the film obtained from chloroform. A very similar pattern to that observed by casting from THF is also found in the difference CD spectrum obtained by subtracting the solid-line from the dotted-line spectrum of Figure 6 (dashed line in Figure 7).

Morphological analysis: Films of **P1** were formed on freshly cut mica under four different casting conditions: from chloroform solution (1 mg in 2.5 mL), under a) high (<1 min) and b) slow (>20 min) evaporation-rate conditions; from c) saturated and d) diluted (1:100 with respect to the saturated) THF solutions under slow (>20 min) evaporation rate conditions. The corresponding topographical images obtained in non-contact mode show four quite different morphologies:

a) Ground roughness around 4 nm (lower than 2 nm in some regions), with grains of between 120 and 300 nm in diameter and heights up to 40 nm (Figure 8).

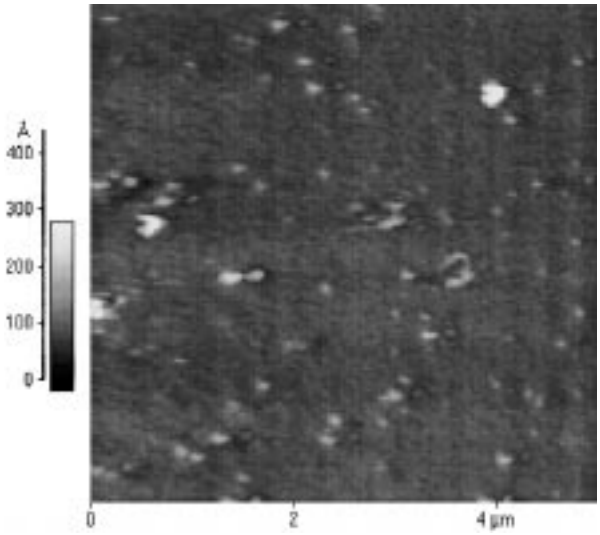

Figure 8. AFM image of **P1** film cast from chloroform under fast evaporation conditions.

b) Astonishingly flat surface, characterised by a roughness lower than 2 Å, with rare grains of around 40 nm in diameter and a few Å high. By passing from noncontact to contact mode, the AFM tip alters the polymer surface and a marked area, whose dimensions match the region scanned in contact mode, is visible on the film surface when the topographical image of a larger area is subsequently acquired (Figure 9).

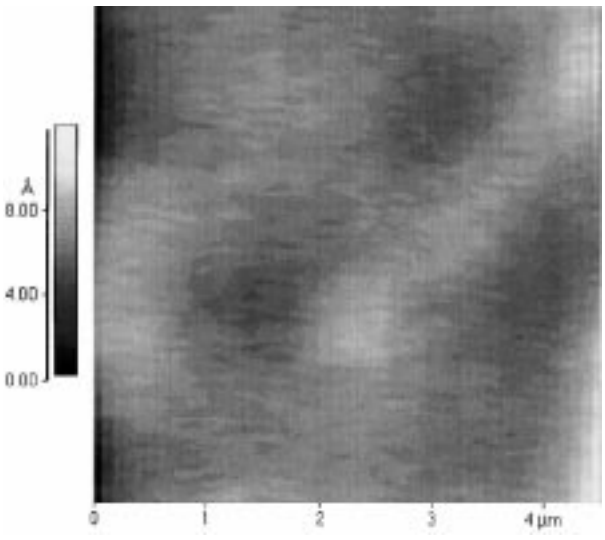

Figure 9. AFM image of **P1** film cast from chloroform under slow evaporation conditions.

c) Grains of various dimensions, with diameters between 1 µm and 10 nm and heights between 50 nm and few Å, over a polymer surface with average roughness of around 4 Å.
d) Rare grains over a film resembling a sort of "neuronal network". The analysis of representative profiles shows the presence of steps with heights of around 45 Å in the border regions, whereas higher profiles are found in the central zones of the "neuronal" patches (Figure 10).

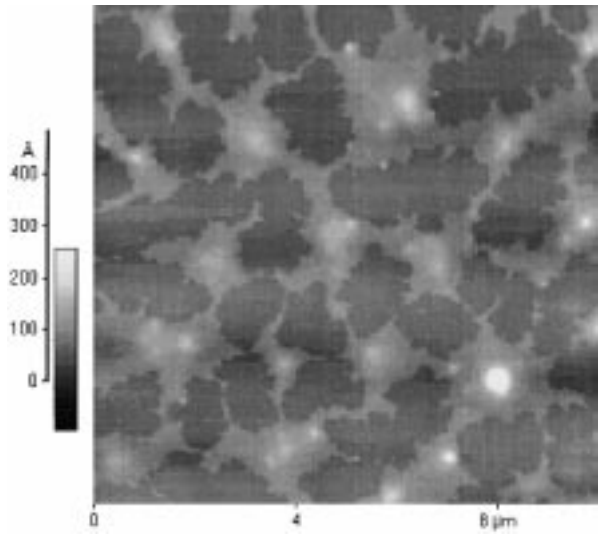

Figure 10. AFM image of **P1** film cast from diluted THF under slow evaporation conditions.

Electrical conductivity: The conductivity values of the p-doped **P1** were obtained by the four-probe method. Films were generated by casting the chloroform solutions onto glass and were oxidised by exposition them to I_2 vapour. The doped films show a conductivity of 1.6 $S\,cm^{-1}$ for **P1**, values similar to those reported for regioregular HH/TT poly[β,β'-bis(alkylsulfanyl)-, (β,β'-dialkyl)- and (β,β'-dialkoxy)bithiophene]s.[10, 12]

Electropolymerisation and electrochemical characterisation: Electropolymerisation of **1** was carried out in a 5 mM monomer solution with tetraethylammonium hexafluorophosphate ($TEAPF_6$) as supporting electrolyte. The resulting polymer is denoted by **PE1**. Figure 11 shows typical cyclic voltammetry curves recorded during the electrogeneration of **PE1** by repeatedly cycling the electrode potential from 0.00 to +1.10 V at a scan rate of 0.05 $V\,s^{-1}$. The increase of the current, scan after scan, is diagnostic of a progressive increase of the quantity of polymer deposited on the electrode surface.

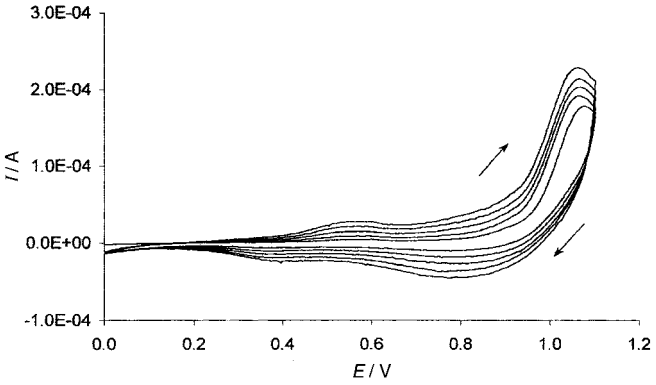

Figure 11. Potentiodynamic growth of **PE1** on a Pt electrode. The curves relative to the first 5 scans are reported: 0.05 $V\,s^{-1}$ potential scan rate; 5 mM monomer, 0.1 M $TEAPF_6$ supporting electrolyte concentrations, CH_3CN solution.

The electrochemical characterisation of the **PE1** films was performed by dipping the modified electrode into a monomer-free solution of CH_3CN containing $TEAPF_6$ as supporting electrolyte. No difference between the electrochemical behaviour of the two polymers was observed. Figure 12 shows the characterisation of the **PE1** film in the anodic region: two distinct anodic-cathodic peak systems are detectable. The less anodic response is indicative of the occurrence of the p-doping process with formation of polarons;[10, 13] this makes the polymer coverage conductive, while the second anodic peak corresponds to the formation of a bipolaron, that is, of a stable two-charge state associated with local geometric

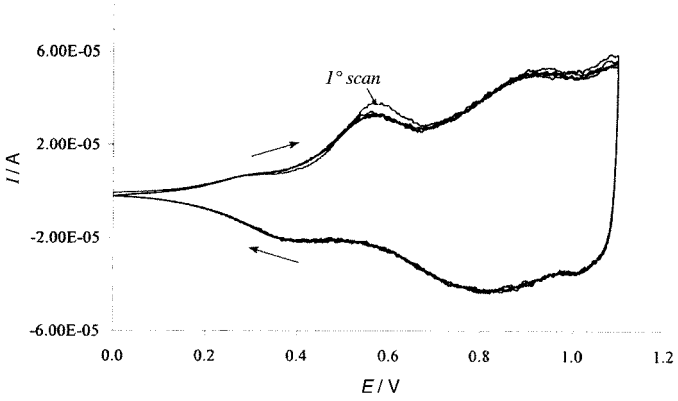

Figure 12. Anodic portion of the cyclic voltammetric curves recorded on a **PE1**-covered Pt electrode: 0.1 M $TEAPF_6$ supporting electrolyte, CH_3CN solution. The first scan cyclic voltammetry plot is clearly distinguishable from the steady-state curves. 0.05 $V\,s^{-1}$ potential scan rate.

0947-6539/01/0703-0680 $ 17.50+.50/0 *Chem. Eur. J.* **2001**, *7*, No. 3

distortions in the polymeric chains. In the backwards scan, two cathodic peaks, associated with the subsequent neutralisation of the two doping states, are detected.

An interesting, small band gap, suggested by the low value (ca. 1.90 V) of the difference between the onset potentials of the anodic and cathodic peaks,[14] allows the observation of a n-doping process in the cathodic region. A de-doping process, associated with a cathodic peak at about -1.85 V, is seen to occur in correspondence to a broader anodic backwards peak. As shown in Figure 13, a different cathodic behaviour is

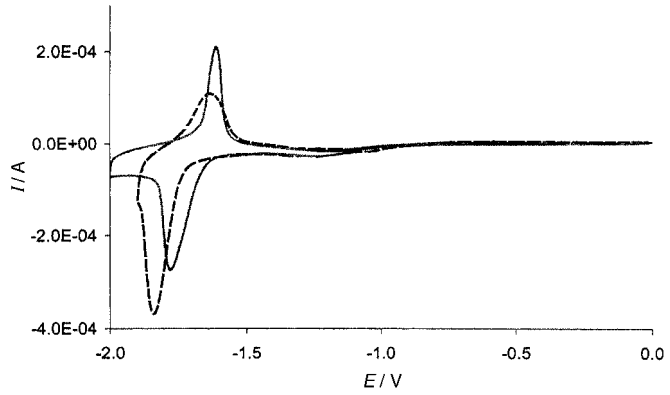

Figure 13. Cathodic portion of the cyclic voltammetric curves recorded on a **PE1**-covered Pt electrode. Different electrochemical behaviour is found in $TEAPF_6$ (----) and in $TBAPF_6$ (——) supporting electrolyte. 0.05 V s^{-1} potential scan rate.

exhibited on varying the supporting electrolyte, depending on the cation dimension. In particular, in experiments carried out with tetrabutylammonium hexafluorophosphate ($TBAPF_6$), two significant differences are observed: the n-doping process takes place at less anodic potentials[15] and the de-doping process occurs with a sharper peak. The current-potential curves recorded over the whole analysed potential interval are reported in Figure 14.

Similar electrochemical characterisation was also carried out on chemically synthesised polymers that were deposited on a platinum electrode by dissolving them in chloroform and

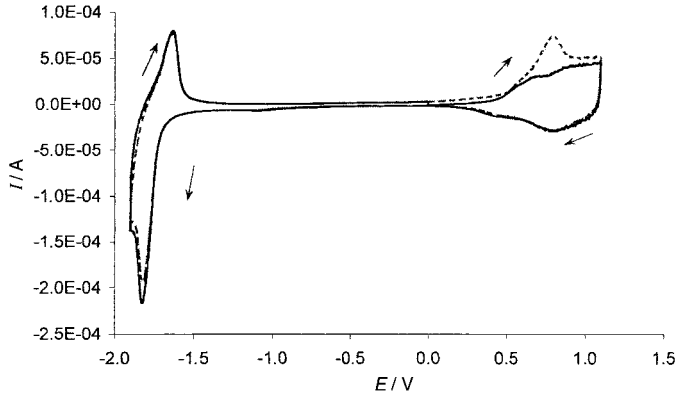

Figure 14. Cyclic voltammetric curves recorded on the polymer **PE1** coated electrode in the potential region where both p- and n-doping take place. The starting potential is -0.20 V for the first anodic scan (——). The dashed line is relative to the second scan, starting when the whole cycle, including cathodic potentials, had been completed. 0.05 V s^{-1} potential scan rate.

permitting a slow evaporation of the solution onto the electrode. This was then dipped into a CH_3CN solution with $TEAPF_6$ as supporting electrolyte. Voltammetric curves very similar to those of the electrogenerated polymer are obtained, both in the anodic and in the cathodic ranges.

In order to estimate the distribution of the molecular weights of the electrogenerated polymer, relatively large amounts were collected by a number of depositions and subsequent dissolutions of the films obtained. Two different procedures can be used to electrogenerate polymer coatings, that is, potentiodynamic and potentiostatic growth. The first one, described in the first part of this section, occurs during a continuously varying potential scan, while the second one requires the electrode to be polarised at a fixed potential which permits monomer oxidation, in this case $+1.10$ V (see Figure 11). To estimate the possible dependence of the weight distribution on the electrogeneration technique followed, tests were performed under both conditions, with a 10 mM monomer concentration. No significant dependence of the molecular-weight distribution on either of the growing variables explored could be ascertained, in either case M_w and M_n in the range 20000–30000 and 8000–9000, respectively, were obtained. This result agrees perfectly with that found for poly[4,4′-bis(butylsulfanyl)-2,2′-bithiophene], in which neither the concentration nor the electrogeneration method has been found to affect the molecular weight distribution.[16]

Discussion

The analysis of UV/Vis, CD and AFM data seems to give significant hints about the self-organisation properties of regioregular PTs, both in solution and in the solid state. As far as the behaviour in solution is concerned, the UV/Vis measurements reported here have shown that solvatochromism can be induced in **P1** not only by polar poor solvents, such as the widely used methanol, but also by apolar poor solvents, such as *n*-hexane. In this latter case, higher ratios for poor (*n*-hexane) to good (chloroform) solvent, with respect to the classical chloroform/methanol mixtures, have to be used in order to induce aggregation.

Two different models can be found in the literature[4a, 6, 11a, 17] to explain the solvatochromic and thermochromic behaviour of regioregular HT or HH/TT PTs. One model considers an intrachain mechanism, based on the existence of an equilibrium process between an ordered, more extensively conjugated, rod-like form that is present in poor solvents or at low temperature, and a disordered, less conjugated, coil-like form that prevails in good solvents and at high temperature and absorbs at a shorter wavelength. The second model considers the formation, in poor solvents or at low temperature, of aggregates in suspension that are in equilibrium with the polymer in solution. This is an interchain mechanism that can be influenced by intrachain phenomena. In principle, microcrystallisation should only occur after the polymer has transformed into a more ordered conformation, but it is not clear yet whether the more ordered conformation is actually induced in regioregular PTs by non-solvents or if

the polymers possess a highly stiff structure even in good solvents, as recently suggested by Yamamoto et al.[6] In this last hypothesis, the bathochromic shift and the vibronic structure observed on passing from chloroform solutions to colloids and films have been attributed to the formation of π-stacked structures. This represents quite a different interpretation of the UV/Vis spectra of PTs. Actually, the vibronic structure is usually interpreted as a symptom of the stiffness of the PT backbone[4c, 5] and is absent in chloroform solution. Moreover, the large red shift consequent to aggregation is not compatible with *H*-type aggregates,[18] as implied by Yamamoto's discussion, but rather with conformational changes[19] and with *J*-type aggregates. These are characterised by a sharp band at longer wavelengths and by a broader one (more or less allowed) at shorter wavelengths, due to exciton coupling.[18, 20] UV/Vis spectra of **P1** in poor solvents and of regioregular PTs indeed show a better-resolved red-shifted band with vibronic structure, but do not allow us to distinguish the second (broader) band expected at shorter wavelengths. Nevertheless, this second band has been detected through CD spectroscopy in the case of **P1** and other chiral regioregular PTs[4, 5] under aggregation conditions: these findings suggest a *J*-type chiral chromophoric disposition in the aggregate phase. Bisignate CD spectra induced by poor solvents or casting on optically active PTs[4, 5] have already been interpreted as being due to exciton coupling and usually have a Davydov splitting of the same order as the vibronic one. Exciton coupling requires the presence of unconjugated (or loosely conjugated) chromophores in a chiral arrangement with each other.[21] This arrangement can derive from intra- and interchain interactions in aggregate PTs. The base chromophore can be considered to be formed by a number of conjugated thiophene units that belong to nearly planar regions of the main chain. A distorted helical conformation, similar to a folded ribbon with alternate planar and distorted regions, can be suggested in the case of prevalent intrachain chromophoric interactions. A number of possibilities can be hypothesised if interchain interactions dominate. Up to now it is not clear which is the dominant mechanism in PTs,[5b] even though interchain mechanisms have been suggested on the basis of the results of an investigation on model oligothiophenes[22a] and phenylene vinylene oligomers.[22b]

The CD-spectral behaviour of **P1** actually deserves further comment in relation to the different experimental conditions employed. The changes observed in the CD spectra of **P1** upon addition of non-solvents suggest the initial formation of an optically active species common to chloroform/methanol and chloroform/*n*-hexane systems (Figure 4). This converts into a second optically active form (Figure 5) which differs in the two media or, alternatively, into different mixtures of at least two kinds of polymer aggregates. The CD behaviour of **P1** suggests a two-step reorganisation process induced in solution by poor solvents of either polarity. The random, optically inactive, monomeric phase present in good solvents is first converted into a chiral monomeric (or loosely aggregated) phase and then into one or more associate phases.

The presence of more than one single aggregate phase is also strongly suggested by the CD analysis of films obtained under different casting conditions. The results of the comparison of the CD spectra of film cast on glass from a good solvent (chloroform) with those from a poorer solvent (THF) may be interpreted on the basis of the presence of at least two different aggregate forms which exhibit different CD spectra: slow evaporation from a good solvent favours an aggregate phase characterised by a bisignate CD spectrum with a first positive CE, whereas fast evaporation from chloroform or slow evaporation from THF favours an aggregate phase with a first negative CE, which is much higher than in the first case. It is interesting to observe that a CD spectrum of this second type is also obtained from the difference of the two CD spectra in Figure 6. This strongly suggests that slow casting from chloroform solution can also produce films containing two different aggregate phases and that films of different constitutions are produced under similar casting conditions. This last observation is common to various authors.[4b, 23]

AFM morphological analysis can be utilised to investigate the presence of different aggregate phases. Grainy aggregates can be distinguished in the topographical images of films obtained by casting **P1** from chloroform under fast evaporation conditions (Figure 8) or from THF under slow evaporation conditions, whereas an astonishingly flat film surface is found when the film obtained by casting **P1** from chloroform under slow evaporation conditions is analysed (Figure 9). A parallelism between the presence of a very homogeneous aggregate phase and CD spectra of the type of those in Figure 6, and between the grainy structures and CD spectra of the type of those in Figure 7 seems to be present. Nevertheless, it should also be considered that the aggregate phase formed from chloroform through fast evaporation is much less optically active or, more probably, contains a much smaller proportion of optically active form than the film obtained from THF (Figure 7). Furthermore, the latter shows an UV/Vis spectrum different from those of all the aggregate phases reported in this work. To explore the possibility of evidencing a second, less grainy phase in films from THF solution, casting on mica from a very diluted THF solution was attempted. The results are quite amazing: a completely different morphology is evidenced by AFM (Figure 10); this confirms the presence of a second, more homogeneous but not continuous phase. Analysis of the heights in the border regions allows us to estimate that the figure of approximately 45 Å should be a multiple of one relevant molecular dimension. Unfortunately, neither UV/Vis nor CD signals were detected for this sample due to its extreme thinness.

With the aim of comparing electrochemically and chemically synthesised optically active polymers, **P1E** was also analysed through AFM, UV/Vis and CD spectroscopy. As shown in Figure 15, the morphological investigation of **P1E** grown on Pt disk electrode revealed a dunelike surface with a homogeneous texture, without showing any grainy phase. However, the wavy appearance is at least partially due to the non-perfect flatness of the Pt support. The UV/Vis spectrum of **P1E** grown on an ITO (indium tin oxide) covered transparent conducting-glass electrode displays the typical vibronic structure already observed for **P1** films of comparable thickness cast on glass. The corresponding CD spectrum of **P1E** shows a very weak bisignate CE, positive at longer

0947-6539/01/0703-0682 $ 17.50+.50/0 *Chem. Eur. J.* **2001**, *7*, No. 3

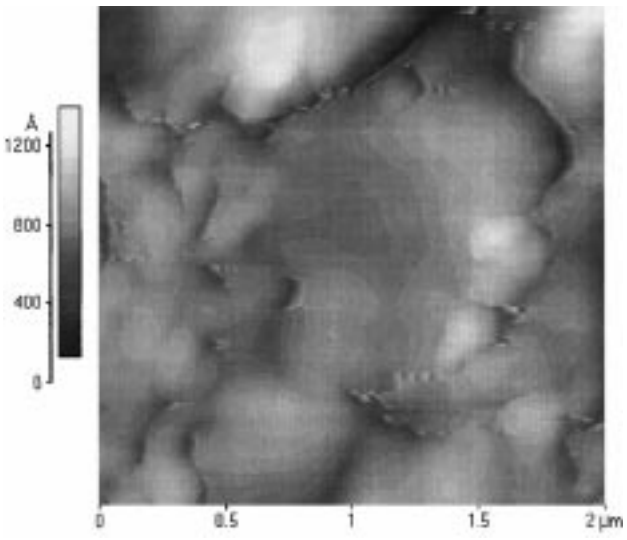

Figure 15. AFM image of **PE1** grown on Pt disk electrode.

wavelengths, similar to that reported in Figure 6 for **P1**. This suggests that an homogeneous phase, with CD characteristics qualitatively similar to those observed in films of **P1** cast on glass and mica, is generated electrochemically. However, the very low optical activity observed is probably due to the fast film formation under the experimental conditions adopted. Further investigations to evaluate the influence of electrogeneration growing conditions on optical activity are in progress.

A first observation that can be drawn from the electrochemical characterisation of both the chemically prepared and the electrogenerated polymers points to the fact that, for both the anodic (p-doping) and the cathodic (n-doping) forward responses, the first curve recorded after a long enough rest time is significantly different from the subsequent ones, recorded by continuous cycling. This behaviour is in good agreement with literature reports on other polymers[24] and fits the requirements of the so-called Electrochemically Stimulated Relaxation Model.[25] This theory suggests a different morphology for the polymer corresponding to different potentials. In particular, the polymer is supposed to become increasingly compact as the negative values of the polarisation potential increase, while it is characterised by a porous structure at sufficiently positive potentials, particularly when it reaches the region at which p-doping actually occurs. The transition from a porous to a compact structure is a slow process, so that increasing the time at negative potentials increases the compactness of the structure.

The cyclic voltammetry curves in Figure 14 show notable differences in the anodic region that depend on whether the deposit had not been previously n-doped or whether, when a whole potential cycle had been completed, enough sufficiently cathodic potentials had been crossed. In particular, in the latter case, only one much sharper and more anodic peak is recorded; once more this difference in behaviour can be explained by realising that more close packing of the polymeric chains occurs when quite negative potentials are reached; this makes the penetration of anionic counterions into the polymer film when the p-doping region is reached more difficult. Detailed studies to account for the dependence on morphology of the electrical properties of these and of other polythiophenes are in progress in our laboratories.

Conclusion

We have characterised, through spectroscopic, electrochemical, surface analysis and M_W determination, a new HH/TT polythiophene **P1** with (*S*)-2-methylbutylsulfanyl chains that was synthesised by both chemical and electrochemical methods. The aim was to gain a better insight into the aggregation processes of PTs, which are supposed to be closely related to the solvato-, thermo-, photo- and electrochromic properties as well as to the electrical conductivity of this class of compounds. Analysis of the CD and AFM spectra of the optically active **P1** shows that at least two different aggregate phases, one with homogeneous and the other with grainy characteristics, are present in the solid state. These phases exhibit different CD and UV/Vis spectra and different morphology. They are formed in various relative proportions, which depend on the experimental conditions. They are of opposite chirality, in the hypothesis of exciton coupling, but it should be underlined that their CD spectra are not related to each other as mirror images. More than two aggregate phases are also formed by adding poor solvents (methanol and *n*-hexane) to a solution of **P1** in chloroform. The CD spectra of the aggregate phases obtained in chloroform/methanol mixtures are very close to the mirror image of the CD spectrum of the film produced by slow casting from chloroform; this suggests an opposite chirality of the chromophore arrangement in these two particular cases. Further experimental as well as theoretical studies are necessary in order to understand the relationship between the type and size of aggregates evidenced by AFM and the parameters that influence the shape, size and sign of the CD signals.

Experimental Section

General techniques: All air- or moisture-sensitive reactions were performed under prepurified nitrogen with dry glassware. Tetrahydrofuran (THF) was distilled from sodium and benzophenone prior to use. Pyridine, chloroform and nitromethane were dried by standard procedures. Iron(III) chloride was purchased from Fluka and dried under vacuum. Melting points (Buchi apparatus) and boiling points are uncorrected.

GPC was carried out by using a Waters Millipore 590 equipped with a TSK gel G4000HXL column and a Perkin-Elmer LC95 UV/Vis spectrophotometer detector, with THF as eluent. The average molecular weights were calculated by using a calibration curve of monodisperse polystyrene standards.

NMR spectra were recorded on a Bruker AMX 400 operating at 400.13 and 100.61 MHz for ^{1}H and ^{13}C, respectively. The residue signal of $CHCl_3$ at $\delta = 7.26$ was used as reference for the proton chemical shifts in $CDCl_3$ solutions and the ^{13}C signal of $CDCl_3$ at $\delta = 77.0$ as reference for carbon chemical shifts. HMQC parameters for aromatic and aliphatic regions are: spectral width (f2) at $\delta = 1-4$; 512–2k points; spectral width (f1) at $\delta = 25-150$; 64–256 t1 increments with 192–128 scans per t1 value; relaxation and evolution delays = 0.2 s and 50 ms, respectively; zero filling in f1 and f2 and sine function in f1 and f2 were applied before Fourier transformation.

FT-IR spectra were recorded by using a Perkin-Elmer i-Series 2000 FT-IR microscope. CD spectra and UV/Vis spectra on 11.0 mg dm^{-3} solutions of **P1** were performed on a JASCO J-710 spectropolarimeter with 1 cm path length.

Atomic force microscopy: 256 × 256 pixel images were recorded with a Park Autoprobe CP scanning probe microscope equipped with silicon cantilevers with sharp conical tips (Ultralever) operating in non-contact mode and at resonance frequencies in the range 200 – 300 kHz.

Fast casting was obtained by evaporating solutions of **P1** onto freshly cut mica surfaces (AFM) or onto glass (CD and UV/Vis) in air. Slow evaporation was obtained in a solvent-saturated atmosphere.

The electrical resistance was measured by using a Kuliche & Soffa series 333 four-point probe. The thickness of the thin films was measured by an Alpha Step-Tensor 200.

Electropolymerisation and electrochemical characterisation of both electrogenerated and chemically synthesised polymers were performed by using an Autolab PGSTAT 30 Electrochemical Instrument. All electrochemical tests were carried out in a single-compartment, three-electrode cell at room temperature and under a nitrogen atmosphere. Platinum disk electrodes (Metrohm), with 0.07 cm^2 and about 3 cm^2 geometric areas, and an ITO covered glass electrode that is transparent at UV/Vis radiations were used as working electrodes in the different electrochemical characterisations. The counter electrode was a glassy carbon-rod electrode (Metrohm). The working electrode was polished with 1 and 0.3 μm alumina powder and then rinsed with distilled water in an ultrasonic bath for 5 minutes before use. All potential values are referenced to an aqueous saturated calomel electrode (SCE, Amel).

All the experiments were carried out in acetonitrile solvent (Aldrich, +99.8% pure, anhydrous, packaged under nitrogen) by using 0.1M tetrabutylammonium hexafluorophosphate ($TBAPF_6$, Fluka, ≥99%) or 0.1M tetraethylammonium hexafluorophosphate ($TEAPF_6$, Fluka, ≥99%) as supporting electrolyte.

The polymer for AFM measurements was grown on Pt disk electrode (3 cm^2 area) under potentiodynamic conditions (4 scans from 0 to 1.10 V, 0.05 V s^{-1} scan rate), with a 5 mM monomer and 0.1M $TEAPF_6$ supporting electrolyte. The polymer for spectroscopic characterisations was synthesised onto ITO glass (20 scans from 0 up to +1.25 V, higher uncompensated resistance being present), the other experimental conditions being the same.

(*S*)-(+)-1-Bromo-2-methylbutane: Phosphorus tribromide (24.6 g, 91 mmol) was added dropwise (2 h) to a stirred solution of (*S*)-(−)-2-methylbutane-1-ol (Aldrich) (20.0 g, 226 mmol), $[\alpha]_D^{23} = -5.8$ ($c = 1.3$ in $CHCl_3$), in dry pyridine (6.8 g, 78.4 mmol) at 0 °C. The reaction mixture was stirred for 2 h at this temperature, for 30 min at 10 °C and was left to stand overnight in the refrigerator. The crude product was distilled at 150 mm Hg and dissolved in light petroleum (50 mL, b.p. 40 – 70 °C). The solution was washed successively with water (40 mL), NaOH (aq) (5%, 15 mL), H_2SO_4 (aq) (10%, 15 mL), concentrated H_2SO_4 (10 mL) and water (30 mL). The organic phase was dried (Na_2SO_4) and evaporated. The residue was short-path distilled to give the (*S*)-(+)-1-bromo-2-methylbutane. Yield: 22.8 g, 66%; b.p. 122 – 123 °C at 760 mm Hg; $[\alpha]_D^{20} = +4$ ($c = 1.1$ in $CHCl_3$) (lit. b.p. 69 °C at 135 mm Hg $[\alpha]_D^{25} = +4.05$ ($CHCl_3$) ref. [26]; ^{1}H NMR (400 MHz, $CDCl_3$, TMS): $\delta = 3.39$ (dd, $^2J = -9.8$ Hz, $^3J = 5.9$ Hz, 1H; H1b), 3.38 (dd, $^2J = -9.8$ Hz, $^3J = 5.2$ Hz, 1H; H1a), 1.7 (m, $^3J = 5.8$ Hz, $^3J = 5.2$ Hz, $^3J = 6.6$ Hz, 1H; H2), 1.5 (m, $^2J = -12.4$ Hz, $^3J = 5.8$ Hz, $^3J = 7.4$ Hz, 1H; H3b), 1.3 (m, $^2J = -12.4$ Hz, $^3J = 5.2$ Hz, $^3J = 7.4$ Hz, 1H; H3a), 1.0 (d, $^3J = 6.6$ Hz, 3H; C2-H_3), 0.9 (t, $^3J = 7.4$ Hz, 3H; C4-H_3).

(*S*)-(+)-2-Methylbutyl-*S*-thioacetate: This compound was obtained from (*S*)-(+)-1-bromo-2-methylbutane (9.35 g, 62 mmol) according to ref. [8]. For the racemic compound: 7.3 g, 80%; b.p. 85 – 87 °C at 29 mm Hg; $[\alpha]_D^{20} = +15$ ($c = 1.0$ in $CHCl_3$); ^{1}H NMR (400 MHz, $CDCl_3$, TMS): $\delta = 2.93$ (dd, $^2J = -13.2$ Hz, $^3J = 5.7$ Hz, 1H; H1b), 2.75 (dd, $^2J = -13.2$ Hz, $^3J = 6.9$ Hz, 1H; H1a), 2.35 (s, 3H; CH_3CO), 1.56 (m, $^3J = 6.6$ Hz, $^3J = 6.9$ Hz, $^3J = 5.7$ Hz, 1H; H2), 1.42 (m, $^2J = -13.4$ Hz, $^3J = 5.9$ Hz, $^3J = 7.4$ Hz, 1H; H3b), 1.21 (m, $^2J = -13.4$ Hz, $^3J = 6.5$ Hz, $^3J = 7.4$ Hz, 1H; H3a), 0.93 (d, $^3J = 6.6$ Hz, 3H; C2-H_3), 0.90 (t, $^3J = 7.4$ Hz, 3H; C4-H_3); elemental analysis calcd (%) for $C_7H_{14}OS$ (146.26): C 57.49, H 9.65, O 10.94, S 21.92; found C 57.54, H 9.48, S 22.15.

(+)-Bis[(*S*)-2-methylbutyl]disulfide: This compound was obtained from (*S*)-(+)-2-methylbutyl-*S*-thioacetate (7.2 g, 49 mmol) according to the method described in ref. [8]. For the racemic compound: 4.0 g, 79%; b.p. 89 – 91 °C at 2 mm Hg; $[\alpha]_D^{20} = +85.8$ ($c = 0.9$ in $CHCl_3$); ^{1}H NMR (400 MHz, $CDCl_3$, TMS): $\delta = 2.74$ (dd, $^2J = -12.8$ Hz, $^3J = 5.9$ Hz, 1H; H1b), 2.54 (dd, $^2J = -12.8$ Hz, $^3J = 7.4$ Hz, 1H; H1a), 1.72 (m, $^3J = 6.6$ Hz, $^3J = 7.4$ Hz, $^3J = 5.9$ Hz, 1H; H2), 1.50 (m, $^2J = -13.0$ Hz, $^3J = 5.2$ Hz, $^3J = 7.4$ Hz, 1H; H3b), 1.22 (m, $^2J = -13.0$ Hz, $^3J = 6.8$ Hz, $^3J = 7.4$ Hz, 1H; H3a), 0.99 (d, $^3J = 6.7$ Hz, C2-H_3), 0.91 (t, $^3J = 7.4$ Hz, 3H; 3H; C4-H_3); elemental analysis calcd (%) for $C_{10}H_{22}S_2$ (206.40): C 58.19, H 10.74, S 31.07; found C 58.45, H 10.45, S 31.92.

(+)-4,4′-Bis[(*S*)-2-methylbutylsulfanyl]-2,2′-bithiophene (1): A solution of 4,4′-dibromo-2,2′-bithiophene[7] (1.53 g, 4.7 mmol) in dry THF (7.6 mL) was added dropwise (20 min) at a temperature of between −60 and −50 °C to a solution of butyllithium (2.1M, 7.8 mL, 10.3 mmol) in dry THF (9.3 mL) at −70 °C. The reaction mixture was stirred for 20 min at −50 °C, and then the temperature was raised to −20 °C. A solution of (+)-bis[(*S*)-2-methylbutyl]disulfide (3.9 g, 18.9 mmol) in dry THF (1.0 mL) was added in one portion, and the temperature allowed to rise to −5 – 0 °C. This temperature was maintained for 1 h, then water (20 mL) and diethyl ether (30 mL) were added. The aqueous layer was separated and extracted with diethyl ether (50 mL). The combined organic extracts were washed successively with NaOH (aq) (10%, 15 mL) and water (15 mL) and dried over $MgSO_4$. The volatile materials were carefully removed under reduced pressure and the crude oil was dissolved in pentane (5 mL). The precipitate obtained by cooling the solution to −5 °C was allowed to settle and crystallised from isopropyl alcohol to give the chiral dimer **1**. Yield: 0.45 g, 26%; m.p. 44 °C; $[\alpha]_D^{20} = +37.5$ ($c = 1.1$ in $CHCl_3$); ^{1}H NMR (400 MHz, $CDCl_3$, TMS): $\delta =$ 7.06 (d, $^4J = 1.4$ Hz, 1H; H3), 6.96 (d, $^4J = 1.4$ Hz, 1H; H5), 2.89 (dd, $^2J = -12.4$ Hz, $^3J = 5.7$ Hz, 1H; H1b), 2.70 (dd, $^2J = -12.4$ Hz, $^3J = 7.3$ Hz, 1H; H1a), 1.66 (m, $^3J = 6.6$ Hz, $^3J = 7.3$ Hz, J(H2,H1b) = 5.7 Hz, 1H; H2), 1.53 (m, $^2J = -13.0$ Hz, $^3J = 5.2$ Hz, $^3J = 7.4$ Hz, 1H; H3b), 1.24 (m, $^2J = -13.0$ Hz, $^3J = 6.8$ Hz, $^3J = 7.4$ Hz, 1H; H3a), 1.02 (d, $^3J = 6.7$ Hz, 3H; C2-H_3), 0.90 (t, $^3J = 7.4$ Hz, 3H; C4-H_3); ^{13}C NMR (100 MHz, $CDCl_3$, TMS): $\delta = 137.2$ (C2), 133.6 (C4), 126.0 (C3), 121.3 (C5), 42.0 (C1′), 34.5 (C2′), 28.0 (C3′), 18.7 (C2′-H_3), 10.5 (C4′-H_3); elemental analysis calcd (%) for $C_{18}H_{26}S_4$ (370.64): C 58.33, H 7.07, S 34.60; found C 58.28, H 6.97, S 34.83.

Poly[4,4′-bis[(*S*)-2-methylbutylsulfanyl]-2,2′-bithiophene] (P1): A solution of $FeCl_3$ (0.37 g, 2.3 mmol) in CH_3NO_2 (10 mL) was added dropwise (2 h) to a stirred solution of dimer **1** (0.21 g, 0.60 mmol) in $CHCl_3$ (10 mL) under a flow of dry nitrogen. The greenish mixture was stirred for 20 h at room temperature and evaporated. The residue was stirred (1 h) with HCl-acidified methanol (40 mL). The dark product was centrifuged, washed with methanol and Soxhlet-extracted with methanol (24 h), *n*-pentane (24 h) and $CHCl_3$ (24 h). The purplish $CHCl_3$ solution (200 mL) was concentrated to nearly dryness and methanol (10 mL) was added to give the polymer **P1** (0.12 g, 59%) as a free-standing, easily detachable greenish-golden film on the glassware. This polymeric film is a flexible material that can be cut with scissors and is soluble in common organic solvents such as $CHCl_3$, CH_2Cl_2, CCl_4, CS_2, benzene, toluene and THF at room temperature. ^{1}H NMR (400 MHz, $CDCl_3$, TMS): $\delta = 7.19$ (s, 1H; H3), 2.91 (dd, $^2J = -12.2$ Hz, $^3J = 5.7$ Hz, 1H; H1b), 2.73 (dd, $^2J = -12.2$ Hz, $^3J = 7.5$ Hz, 1H; H1a), 1.64 (m, $^3J = 6.5$ Hz, $^3J = 7.5$ Hz, J(H2,H1b) = 5.7 Hz, 1H; H2), 1.52 (m, 1H; H3b), 1.25 (m, 1H; H3a), 1.00 (d, $^3J = 6.5$ Hz, 3H; C2-H_3), 0.89 (t, $^3J = 7.5$ Hz, 3H; C4-H_3); ^{13}C NMR (100 MHz, $CDCl_3$, TMS): $\delta = 136.1$ (C2), 133.0 (C4), 131.7 (C5), 127.4 (C3), 43.5 (C1′), 34.9 (C2′), 28.6 (C3′), 18.9 (C2′-H_3), 11.3 (C4′-H_3).

Acknowledgement

The authors are grateful to the Italian MURST for financial support. Thanks are due to the Centro Interdipartimentale Grandi Strumenti of the University of Modena for the use of the Bruker AMX-400 WB spectrometer, the Perkin-Elmer i-Series FT-IR and the Park Autoprobe CP scanning probe microscopes. We are grateful to Professor F. Nava for conductivity measurements.

[1] a) D. Fichou, *Handbook of Oligo- and Polythiophenes*, Wiley-VCH, Weinheim, **1999**; b) G. Schopf, G. Koßmehl, *Adv. Polym. Sci.* **1997**, *129*, 143 – 145; c) H. S. Nalwa, *Handbook of Organic Conductive Molecules and Polymers*, *Vol. 2*, Wiley, Chichester, **1997**.

[2] a) R. D. McCullough, R. D. Lowe, M. Jayaraman, D. L. Anderson, *J. Org. Chem.* **1993**, *58*, 904–912; b) T.-A. Chen, X. Wu, R. D. Rieke, *J. Am. Chem. Soc.* **1995**, *117*, 233–244.
[3] L. Schenetti, A. Mucci in *New Advances in Analytical Chemistry*, *Part 1* (Ed.: A.-U. Rahman), Harwood Academic, Amsterdam, **2000**.
[4] a) M. M. Bouman, E. E. Havinga, R. A. J. Janssen, E. W. Meijer, *Mol. Cryst. Liq. Cryst.* **1994**, *256*, 439–448; b) M. M. Bouman, E. W. Meijer, *Adv. Mater.* **1995**, *7*, 385–387; c) B. M. W. Langeveld-Voss, M. M. Bouman, M. P. T. Christiaans, R. A. J. Janssen, E. W. Meijer, *Polym. Mater. Sci. Eng.* **1996**, *37*, 499–500; d) B. M. W. Langeveld-Voss, R. A. J. Janssen, M. P. T. Christiaans, S. C. J. Meskers, H. P. J. M. Dekkers, E. W. Meijer, *J. Am. Chem. Soc.* **1996**, *118*, 4908–4909; e) B. M. W. Langeveld-Voss, E. Peeters, R. A. J. Janssen, E. W. Meijer, *Synth. Met.* **1997**, *84*, 611–614; f) B. M. W. Langeveld-Voss, M. P. T. Christiaans, R. A. J. Janssen, E. W. Meijer, *Macromolecules* **1998**, *31*, 6702–6704.
[5] a) F. Andreani, L. Angiolini, D. Caretta, E. Salatelli, *J. Mater. Chem.* **1998**, *8*, 1109–1111; b) G. Bidan, S. Guillerez, V. Sorokin, *Adv. Mater.* **1996**, *8*, 157–160.
[6] T.Yamamoto, D. Komarudin, M. Arai, B.-L. Lee, H. Suganuma, N. Asakawa, Y. Inoue, K. Kubota, S. Sasaki, T. Fukuda, H. Matsuda, *J. Am. Chem. Soc.* **1998**, *120*, 2047–2058.
[7] U. Folli, F. Goldoni, D. Iarossi, A. Mucci, L. Schenetti, *J. Chem. Res.* **1996**, 69.
[8] P. Dubs, R. Stüssi, *Helv. Chim. Acta* **1978**, *61*, 2351–2359.
[9] A. Bax, R. H. Griffey, B. L. Hawkins, *J. Magn. Reson.* **1983**, *55*, 301–315.
[10] D.Iarossi, A. Mucci, L. Schenetti, R. Seeber, F. Goldoni, M. Affronte, F. Nava, *Macromolecules* **1999**, *32*, 1390–1397.
[11] a) S. D. D. V. Rughooputh, S. Hotta, A. J. Heeger, F. Wudl, *J. Polym. Sci. Polym. Phys. Ed.* **1987**, *25*, 1071–1078; b) W. R. Salaneck, O. Inganäs, B. Thémans, J. O. Nilsson, B. Sjögren, J.-E. Österholm, J.-L. Brèdas, S. Svensson, *J. Chem. Phys.* **1988**, *89*, 4613–4619; c) K. Tashiro, Y. Minagawa, M. Kobayashi, S. Morita, T. Kawai, K. Yoshino, *Synth. Met.* **1993**, *55*, 321–328; d) K. Faïd, M. Fréchette, M. Ranger, L. Mazerolle, I. Lévesque, M. Leclerc, T.-A. Chen, R. D. Rieke, *Chem. Mater.* **1995**, *7*, 1390–1396; e) M. Leclerc, M. Fréchette, J. Y. Bergeron, M. Ranger, I. Lévesque, K. Faïd, *Macromol. Chem. Phys.* **1996**, *197*, 2077–2087; f) M. Leclerc, K. Faïd, *Adv. Mater.* **1997**, *9*, 1087–1094.
[12] a) R. M. Souto Maior, K. Hinkelmann, H. Eckert, F. Wudl, *Macromolecules* **1990**, *23*, 1268–1279; b) K. Faïd, R. Cloutier, M. Leclerc, *Macromolecules* **1993**, *26*, 2501–2507; c) M. Zargóska, B. Krische, *Polymer* **1990**, *21*, 1379–1383.
[13] J. Heinze, *Synth. Met.* **1991**, *41–43*, 2805–2823.
[14] S.-C. Ng, P. Miao, H. S. O. Chan, *Chem. Commun.* **1998**, 153–154.
[15] F. Mohammad, *Synth. Met.* **1999**, *99*, 149–154.
[16] B. Ballarin, F. Costanzo, F. Mori, A. Mucci, L. Pigani, L. Schenetti, R. Seeber, D. Tonelli, C. Zanardi, *Electrochim. Acta*, in press.
[17] a) X. Wu, T.-A. Chen, R. D. Rieke, *Macromolecules* **1996**, *29*, 7671–7677; b) F. Raymond, N. Di Césare, M. Belletête, G. Durocher, M. Leclerc, *Adv. Mater.* **1998**, *10*, 599–602; c) C. Roux, J. Y. Bergeron, M. Leclerc, *Makromol. Chem.* **1993**, *194*, 869–877.
[18] E. G. McRae, M. Kasha in *Physical Processes in Radiation Biology* (Eds.: L. Augenstein, R. Mason, B. Rosenberg), Academic Press, New York, **1964**, p. 23.
[19] N. Di Césare, M. Belletête, M. Leclerc, G. Durocher, *Chem. Phys. Lett.* **1998**, *291*, 487–495.
[20] U. DeRossi, S. Dähne, S. C. J. Meskers, H. P. J. M. Dekkers, *Angew. Chem.* **1996**, *108*, 827–830; *Angew. Chem. Int. Ed. Engl.* **1996**, *35*, 760–763.
[21] a) N. Harada, K. Nakanishi, *Circular Dichroic Spectroscopy*, Oxford University Press, Oxford, **1983**; b) N. Berova, D. Gargiulo, F. Derguini, K. Nakanishi, N. Harada, *J. Am. Chem. Soc.* **1993**,*115*, 4769–4775.
[22] a) B. M. W. Langeveld-Voss, D. Beljonne, Z. Shuai, R. A. J. Janssen, S. C. J. Meskers, E. W. Meijer, J.-L. Bredas, *Adv. Mater.* **1998**, *10*, 1343– ■■; b) E. Peeters, R. A. J. Janssen, S. C. J. Meskers, E. W. Meijer, *Polym. Prep.* **1999**, *40*, 519–520.
[23] a) T. Yamamoto, H. Suganuma, T. Maruyama, T. Inoue, Y. Muramatsu, M. Arai, D. Komarudin, N. Ooba, S. Tomaru, S. Sasaki, K. Kubota, *Chem. Mater.* **1997**, *6*, 1217–1225; b) J. I. Nanos, J. W. Kampf, M. D. Curtis, L. Gonzalez, D. C. Martin, *Chem. Mater.* **1995**, *7*, 2332–2337.
[24] A. Smie, A. Synowczyk, J. Heinze, R. Alle, P. Tschuncky, G. Götz, P. Bäuerle, *J. Electroanal. Chem.* **1998**, *452*, 87–95.
[25] T. F. Otero, H.-J. Grande, J. Rodriguez, *J. Phys. Chem. B* **1997**, *101*, 3688–3697.
[26] P. Salvadori, L. Lardicci, M. Stagi, *Gazz. Chim. Ital.* **1968**, 1400–1416.

Received: June 7, 2000 [F2533]